Anisotropic thermoelectric properties associated with dimensional crossover in quasi-one-dimensional $SrNbO_{3.4+d}$ ($d \sim 0.03$)

W. Kobayashi*
Graduate School of Pure and Applied Sciences, University of Tsukuba, Ibaraki 305-8571 and PRESTO, Japan Science and Technology Agency, Saitama 332-0012, Japan

Y. Hayashi, M. Matsushita, and Y. Yamamoto
Department of Applied Physics, Waseda University, Tokyo 169-8555, Japan

I. Terasaki
Department of Physics, Nagoya University, Nagoya 464-8602, Japan

A. Nakao, H. Nakao, and Y. Murakami
Condensed Matter Research Center and Photon Factory, Institute of Materials Structure Science, High Energy Accelerator Research Organization, Tsukuba 305-0801, Japan

Y. Moritomo
Graduate School of Pure and Applied Sciences, University of Tsukuba, Ibaraki 305-8571, Japan

H. Yamauchi and M. Karppinen
Department of Chemistry, Aalto University, FI-00076 Espoo, Finland

(Received 20 March 2011; revised manuscript received 1 August 2011; published 23 August 2011)

We have grown large single crystals of $SrNbO_{3.4+d}$ ($d \sim 0.03$) with $n = 5$ in the homologous series $Sr_nNb_nO_{3n+2}$ by using a traveling solvent floating-zone method and measured resistivity, thermopower, and thermal conductivity along all crystallographic axes. The thermoelectric properties are found to be highly anisotropic, which reflects a quasi-one-dimensional electronic structure. In particular, the thermopower along the b axis is -170 μV/K at 300 K, which is 1 order of magnitude higher than the -15 μV/K along the a axis and -25 μV/K along the c axis. A possible origin of the high anisotropy in the thermopower is discussed in terms of dimensional crossover associated with a structural modification.

DOI: 10.1103/PhysRevB.84.085118 PACS number(s): 72.15.Jf, 71.10.Pm

I. INTRODUCTION

Thermoelectric oxides are promising materials for recovering electric energy from waste heat. Recent developments in nanotechnology enable the achievement of a thermoelectric performance higher than that of conventional thermoelectrics. Since the enhancement of the dimensionless figure of merit $ZT \equiv \frac{S^2T}{\rho\kappa}$ (S, thermopower; ρ, resistivity; κ: thermal conductivity; and T, temperature) in nanostructures was predicted by Hicks and Dresselhaus in 1993,[1] artificial structures with low dimensionality have been extensively studied.[2] A nanostructure such as a superlattice or nanowire can show good thermoelectric properties owing to the reduced thermal conductivity by phonon scattering at the artificially controlled boundary and the enhanced thermopower by a steep change in the density of states at the Fermi level. Indeed, the Bi_2Te_3/Sb_2Te_3 superstructure exhibits high performance above $ZT = 2.4$,[3] and also recent studies on Si nanowires show a performance 50 times higher than that of bulk Si.[4,5] The two-dimensional (2D) electron gas induced at the interface between $SrTiO_3$ and TiO_2 also displays a high thermopower, of the order of 1 mV/K.[6]

Not only artificial nanostructures but also bulk oxides with a low-dimensional electronic structure have been known to be promising thermoelectric materials since 1997. Layered cobalt oxide Na_xCoO_2 and misfit layered cobalt oxides exhibit a ZT of the order of unity at high temperatures.[7–9] Their large thermopowers are successfully explained by both band calculation[10,11] and the extended Heikes formula.[12] Compared with the extensive study of layered oxides, there has been little research on the thermoelectricity of quasi-one-dimensional (Q1D) oxides,[13–15] because they tend to be insulating even at room temperature and sometimes exhibit a charge density wave (CDW) or spin density wave (SDW) due to the nesting of the sheet-like Fermi surfaces, which is a disadvantage for thermoelectricity.

We have studied thermoelectric properties of Q1D Hollandites $Ba_{1.2}Rh_8O_{16}$ and $K_2Ru_8O_{16}$[16–18]C and found that $Ba_{1.2}Rh_8O_{16}$ exhibits the large power factor ($P \equiv \frac{S^2}{\rho}$) of 30 μW/cm K^2 at 75 K, comparable to that seen in Na_xCoO_2 at 300 K. However, the magnitude of the thermopower is about 20 μV/K at 300 K for both Hollandites, and enhancement of the thermopower due to the Q1D electronic structure was not observed. The low anisotropy in the resistivity ($\rho_\perp/\rho_\parallel \sim 3$ at 300 K) in these systems implies a three-dimensional (3D)-like electronic structure rather than a Q1D one. Thus, a Q1D material with a high anisotropy in conduction is desirable for the enhanced thermopower.

$SrNbO_{3.4}$ with $Nb^{4.8+}$ ($4d^{0.2}$) is a good Q1D conductor.[19] $SrNbO_{3.4}$ belongs to a homologous series, $Sr_nNb_nO_{3n+2}$ ($n = 5$; $Sr_5Nb_5O_{17}$), and is derived from the 3D network

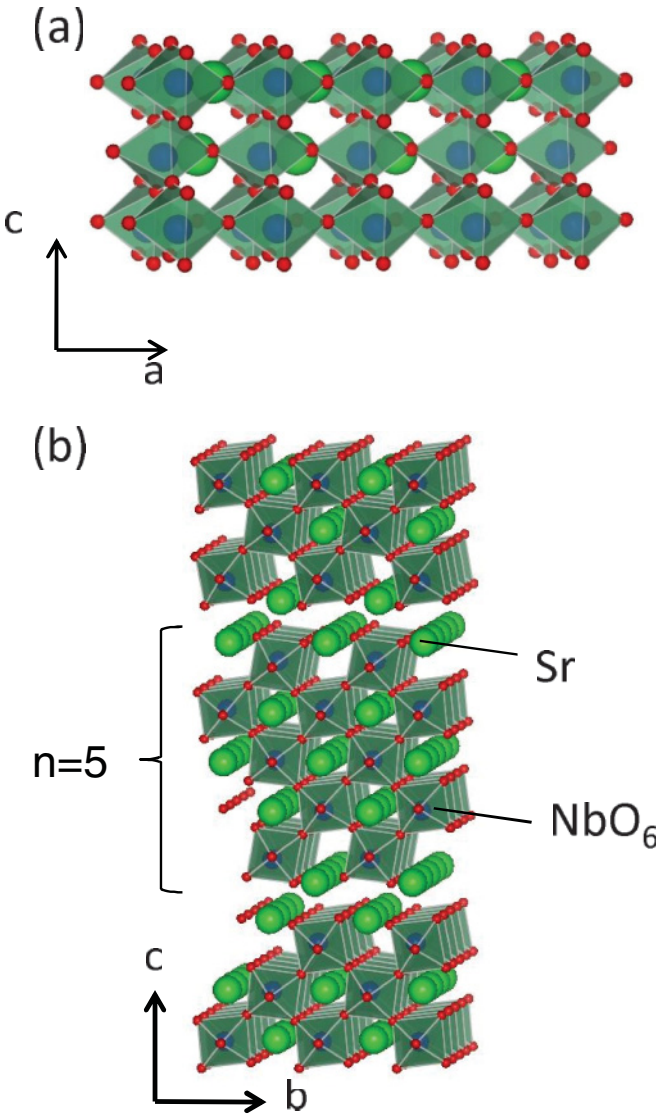

FIG. 1. (Color online) Projection along (a) the *b* axis and (b) the *a* axis of the $SrNbO_{3.4}$ crystal structure.

of the $SrNbO_3$ perovskite structure by separating the NbO_6 octahedra parallel to the (110) planes and introducing additional oxygen.[20] As shown in Fig. 1(a), NbO_6 octahedra form a straight chain structure along the *a* axis, while NbO_6 octahedra form a zigzag path along the *b* axis [see Fig. 1(b)], which realizes high anisotropy even in the *ab* plane. Since the resistivity along the *c* axis is the highest due to the layered structure, the anisotropy in the resistivity becomes $\rho_a:\rho_b:\rho_c = 1:10^2:10^4$.[19] Very recently, Sakai *et al.* have reported anisotropic thermoelectricity in $SrNbO_{3.4}$ and concluded that strong upgrading of the ZT by using pseudo-1D material is not observed.[21] Motivated by Ref. 19, we have grown single crystals of $SrNbO_{3.4+\delta}$, measured the resistivity, thermopower, and thermal conductivity along all crystallographic axes, and analyzed the data combining structural data measured by synchrotron powder x-ray diffraction. The resistivity is found to be 7, 110, and 840 mΩ cm for the *a*, *b*, and *c* axes at 300 K, showing an anisotropy of ∼15 in the *ab* plane. The thermopower along the *b* axis is −170 μV/K, which is 1 order of magnitude higher than those along the other axes. A possible origin of the enhanced thermopower along the *b* axis is discussed in terms of dimensional crossover associated with a structural modification.

II. EXPERIMENTS

High-quality single crystals of $SrNbO_{3.4+d}$ were grown by a traveling solvent floating zone method with a growth velocity of 10 mm/h in a mixed-gas flow of Ar (97%) and H_2 (3%) at 0.2 L/min. Feed rods of fully oxidized $SrNbO_{3.5}$ were prepared by solid-state reaction. Stoichiometric amounts of $SrCO_3$ and Nb_2O_5 were mixed, and the mixture was sintered at 1300 °C for 12 h. Then the product was finely ground, pressed into a bar shape with a 5-mm diameter and 5-cm length, and sintered at 1300 °C for 12 h. Large single crystals with a typical dimension of 5 × 5 × 1 mm^3 were successfully grown.

The x-ray diffraction pattern of the single crystal along the *c* axis was checked using a standard diffractometer with CuKα radiation as an x-ray source in the θ–2θ scan mode (Rigaku MiniFlexII). Synchrotron powder x-ray diffraction measurements at a wavelength of 0.7749 Å were carried out at the BL-8A at the Photon Factory (KEK), controlling the temperature from 80 to 300 K, and structural refinements were performed by Rietveld analysis (RIETAN-FP). The oxygen stoichiometry was determined by means of thermogravimetry (TG) described elsewhere.[22] The orientations of the crystals were determined by backreflection Laue x-ray diffraction.

Resistivity was measured by a four-probe method in a liquid He cryostat. Gold wires were carefully attached to the sample using silver paste (DuPont 4922) as electrodes. Thermopower was measured using a steady-state technique in a liquid He cryostat with a copper-constantan thermocouple to detect a small temperature gradient of about 1 K/cm. Thermal conductivity was measured by a steady-state technique with a chromel-constantan differential thermocouple to detect a temperature gradient. One edge of the crystal was glued to a cold head of a closed cycle refrigerator with varnish (GE 7031), while a resistive heater (∼120 Ω; KYOWA strain gauges) was attached on the opposite edge. The error in the heat current estimation should be below 0.15% using a chromel wire of 50-μm diameter and 2-cm length. To avoid leakage of the heat current by radiation and conduction through the air, we attached a Cu radiation shield and evacuated the air down to 10^{-4} Pa. Heat loss was evaluated to be ∼16% along the *c* axis, which is greater than the ∼8% along the *a* axis and ∼5% along the *b* axis at 300 K.

III. RESULTS AND DISCUSSION

A. Sample characterization and transport properties

Figure 2(a) shows the x-ray diffraction pattern of a $SrNbO_{3.4+d}$ single crystal along the *c* axis. (00*l*) peaks are clearly observed. The *c*-axis length was evaluated to be 32.47 Å, which is very close to that reported in the preceding work.[19] As shown in Fig. 2(b), the synchrotron x-ray diffraction pattern of a ground single crystal was well fitted by orthorhombic symmetry (*Pnnm*; Int. Tables A-58-1) with lattice parameters of $a = 3.988$ Å, $b = 5.676$ Å, and $c = 32.467$ Å.[19] From TG measurement, the oxygen content

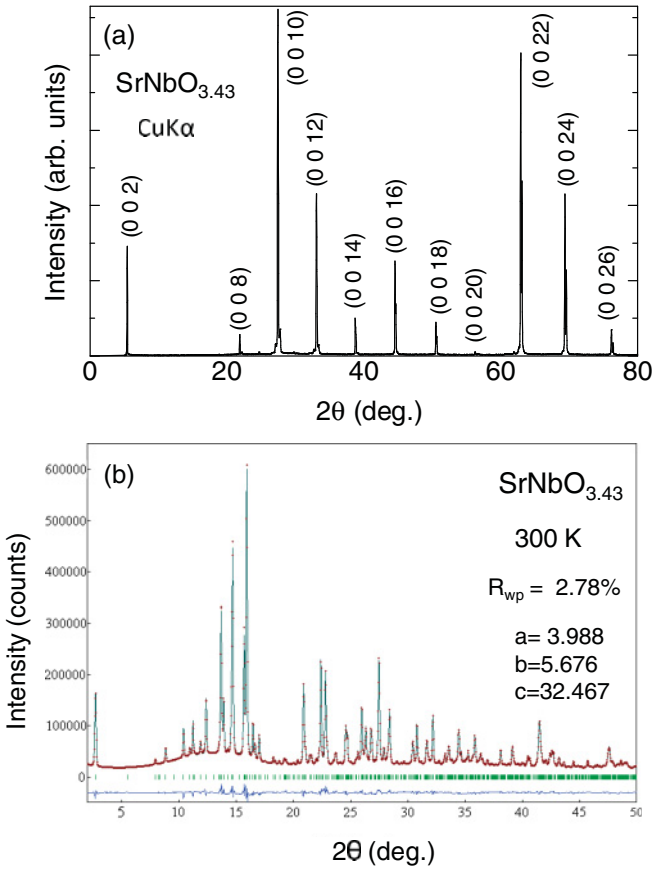

FIG. 2. (Color online) (a) X-ray diffraction pattern along the c axis and (b) synchrotron powder x-ray diffraction pattern of a ground single crystal.

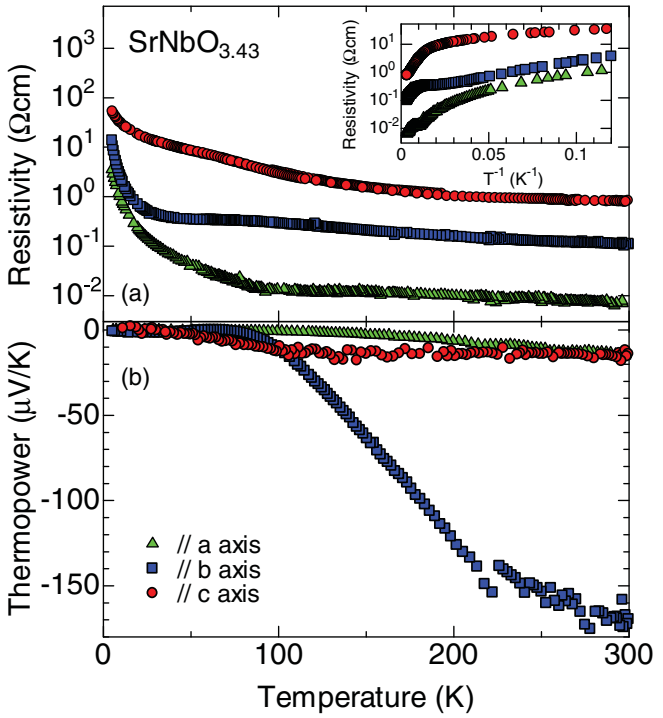

FIG. 3. (Color online) Temperature dependence of (a) resistivity and (b) thermopower.

d was evaluated to be 0.03. Accordingly, we use $SrNbO_{3.43}$ as the chemical formula hereafter.

Figure 3(a) shows the temperature dependence of the resistivity along all the crystallographic axes (ρ_a, ρ_b, and ρ_c). The magnitude of the resistivity is 7, 110, and 840 mΩ cm at 300 K for the a, b, and c axes, respectively, showing an anisotropy of $\rho_b/\rho_a \sim 15$ in the ab plane, and $\rho_b/\rho_a \sim 120$ in the ac plane. This anisotropic behavior is the same as seen in $SrNbO_{3.41}$. On the other hand, the magnitudes of the resistivities are several times larger than those of $SrNbO_{3.41}$.[23] This difference is caused by the different carrier concentrations, namely, different valences of Nb ions, $Nb^{4.82+}(4d^{0.18})$ for $SrNbO_{3.41}$ and $Nb^{4.86+}(4d^{0.14})$, for $SrNbO_{3.43}$. Indeed, $SrNbO_{3.45}$, with the higher valence of $Nb^{4.9+}(4d^{0.1})$, exhibits resistivities higher than those of $SrNbO_{3.43}$.[24] As shown in the inset in Fig. 3(a), the temperature dependence of the resistivity is described over a wide range of temperatures by the activation transport as $\rho = \rho_0 \exp(E_g/k_B T)$, where ρ_0, E_g, and k_B represent a constant, the activation energy, and the Boltzmann constant. At around 300 K, E_g was evaluated to be 29.7, 26.4, and 19.9 meV for the a, b, and c axes, respectively. With decreasing temperature, $\rho(T)$ changes at around $T^* = 100$ K and the quite low E_g of 1–2 meV was found for all axes below 20 K. A similar result has been reported for $SrNbO_{3.41}$.[19,23]

Figure 3(b) shows the temperature dependence of the thermopower along the a, b, and c axes (S_a, S_b, and S_c), respectively. The thermopower is negative along all the directions, and the magnitude (of the thermopower) along the b axis is found to be 170 μV/K at 300 K, which is about 10 times higher than the 15 μV/K for the a axis and 20 μV/K for the c axis. Though 1D conductors generally show such an anisotropic thermopower due to the anisotropic electronic structure,[25,26] we would like to emphasize that the coexistence of a high thermopower that is typical for a semiconductor and a low thermopower for a conventional metal is a significant characteristic of this system. The temperature dependence of the thermopower seems to change at around $T^* = 100$ K, where $\rho(T)$ displays the change in the activation energy. In particular, S_b increases significantly above T^*. According to the Mott formula,[27] S is described as $S = \frac{\pi^2}{3}\frac{k_B}{e}k_B T(\frac{\partial ln\sigma}{\partial E})_{E=E_F}$, where e and σ represent the electron charge and electric conductivity, respectively. Here, the conductivity σ is related to the electronic state at the Fermi level.[27] Thus, the change in $\rho(T)$ and $S(T)$ at T^* implies a modification of the electronic state of $SrNbO_{3.43}$. Similar behaviors are also observed in the layered-cobalt oxysulfide $Sr_2Cu_2CoO_2S_2$, in which electronic inhomogeneity is proposed at about the temperature where the thermopower increases,[28] and in the Q1D oxide $PrBa_2Cu_4O_8$, in which dimensional crossover is suggested.[29] Note that the thermopower along the c axis differs in magnitude from that reported in Ref. 21. The difference could originate from the different density of states along the c axis.

Figures 4(a)–4(c) show the temperature dependence of the thermal conductivity along the a, b, and c axes (κ_a, κ_b, and κ_c), respectively. As seen for ρ and S, κ also exhibits a high anisotropy; κ_a is 6.0 W/mK at 300 K, which is 3 times larger than the κ_b of 2.1 W/mK and 10 times larger than

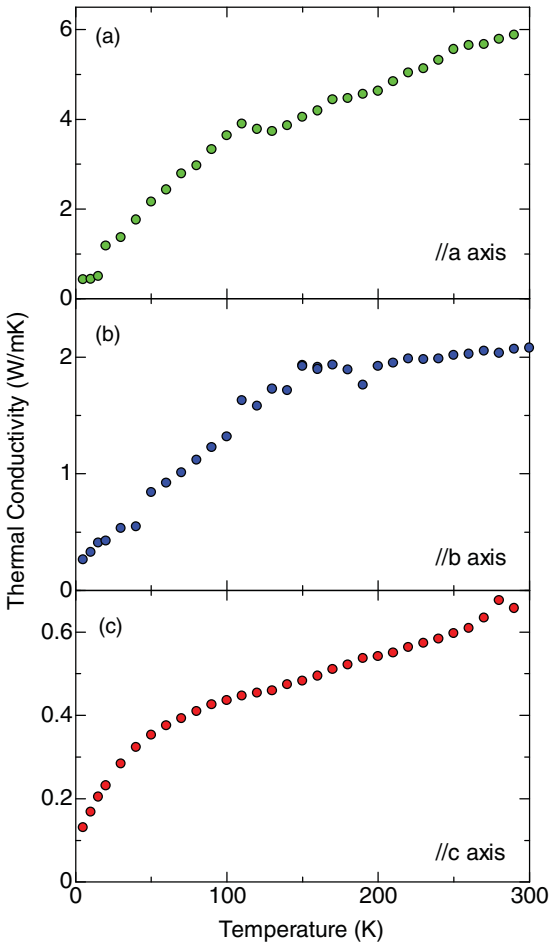

FIG. 4. (Color online) Temperature dependence of the thermal conductivity along (a) the *a* axis, (b) the *b* axis, and (c) the *c* axis.

the κ_c of 0.6 W/mK. The total thermal conductivity κ_{tot} is the sum of the lattice thermal conductivity κ_{ph} and the electron thermal conductivity κ_{el} ($\kappa_{tot} = \kappa_{ph} + \kappa_{el}$). In this system, κ_{el} is negligibly small because of the rather low electric conductivity. As a result, this anisotropy comes from κ_{ph}. Such a high anisotropy in κ_{ph} is also seen in the 2D superlattice or Q1D organic compound, where the mean free paths of phonons are different along crystallographic axes.[30,31] As shown in Fig. 1(a), phonons may easily propagate along the *a* axis due to straight -Sr-Sr-Sr- and -Nb-O-Nb-O- networks, while a zigzag network along the *b* axis and a layered structure along the *c* axis can be effective scatterers. The possibility that there is also substantial anisotropy in the phonon dispersion (anisotropy in sound velocity) is an open question. In addition to the anisotropy, we would like to emphasize that the phonon mean free path is very weakly temperature dependent. The thermal conductivity data show no peak structure at low temperatures, which implies that the phonon-phonon scattering rate is high. The high scattering rate can be attributed to defects in the crystal. Table I lists S, ρ, κ, and dimensionless figure of merit ZT at 300 K along all crystallographic directions. Owing to the high thermopower along the *b* axis, ZT reaches 3.7×10^{-3} along the *b* axis.

TABLE I. S (μV/K), ρ (mΩcm), κ (W/mK), and ZT values at 300 K.

Axis	S	ρ	κ	ZT
a	−15	7	6.0	1.6×10^{-4}
b	−170	110	2.1	3.7×10^{-3}
c	−20	840	0.6	2.4×10^{-5}

B. Structure-related thermoelectric properties

As shown in Fig. 3, $SrNbO_{3.43}$ changes its thermoelectric properties below 150 K: (1) the activation energy decreases with decreasing temperature; and (2) $\frac{dS}{dT}$ decreases with decreasing temperature, in particular, along the *b* axis. These results indicate that $SrNbO_{3.43}$ undergoes a metallic-like state at low temperatures compared with the weak semiconducting state above 150 K. This situation is rather strange, because Q1D material often displays a CDW or SDW state associated with insulating behavior, which cannot explain our observations. Recently, Campos *et al.* revealed that the small gap in resistivity at low temperatures is not attributable to CDW, showing heat capacity and thermal-expansion-coefficient measurements, and reported that power-law fitting is reasonable, indicating a possible signature of Luttinger liquid behavior.[23]

To elucidate the possible origin of the crossover, the crystal structure was analyzed by Rietveld refinement using synchrotron powder x-ray diffraction data between 70 and 300 K. Figure 5 shows the temperature dependences of the lattice parameters. A structural phase transition was not observed in the measured temperature range, though the temperature dependence of the lattice parameters changes slightly below 150 K. This behavior is consistent with the temperature dependence of the linear thermal expansion of $SrNbO_{3.41}$.[23]

Now we mainly focus on the transport properties along the *b* axis where the thermopower rapidly increases at around T^*. Figure 6(a) depicts the projection along the *a* axis of $SrNbO_{3.43}$. There are three crystallographic Nb sites [Nb(1), Nb(2), and Nb(3)] in $SrNbO_{3.43}$. According to the band calculations,[32,33] the predominant contribution to the density of states at E_F is attributed to the Nb(1) site situated in the middle of the slab [see Fig. 6(a)], while the contributions of the other two Nb sites are considerably small. The $Nb(1)O_6$ octahedra are the least distorted ones, with the Nb atoms situated in the center of the octahedra, while the Nb(2) and Nb(3) atoms are considerably displaced away from the central position of the NbO_6 octahedron. Consequently, the Q1D transport is related to the central chain with the least distorted octahedra in the slab. Thus, the temperature dependences of the bond lengths of Nb-O and/or Nb-O-Nb bond angles of $Nb(1)O_6$ and $Nb(3)O_6$ octahedra are important for understanding the transport properties along the *b* axis.

Figures 6(b)–6(e) show the temperature dependence of Nb(1)-O(x) ($x = 1,2$) and Nb(3)-O(x) ($x = 1,2$) distances and Nb(1)-O(1)-Nb(3) and Nb(1)-O(2)-Nb(3) angles, respectively. Both angles decrease monotonically , which signifies rotations of NbO_6 octahedra with decreasing temperature. On the other hand, Nb(1)-O(2) and Nb(3)-O(2) bond lengths change significantly at around 150 K. Now let us focus on Fig. 6(b),

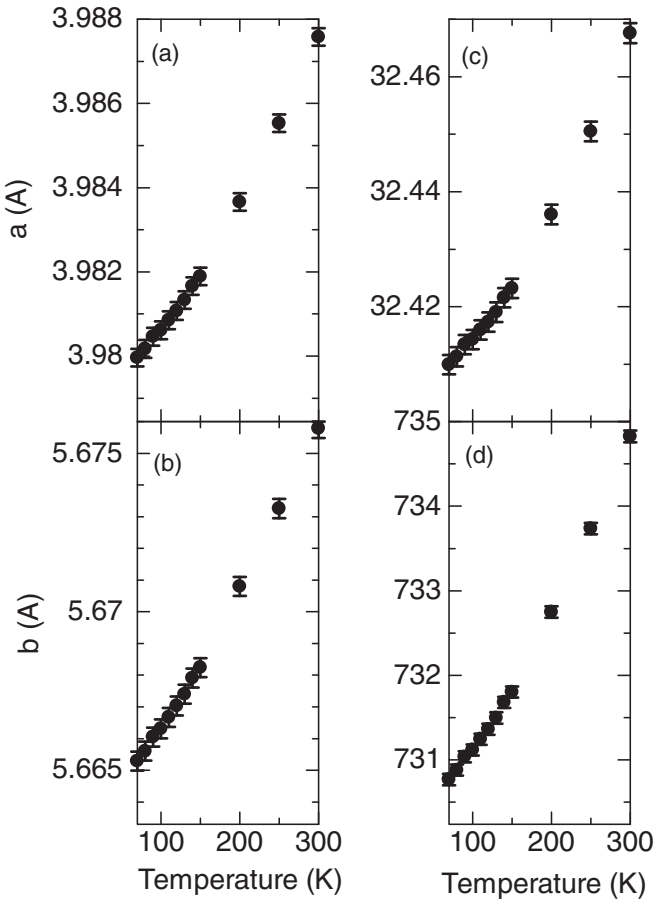

FIG. 5. Temperature dependences of (a–c) lattice parameters and (d) unit cell volume.

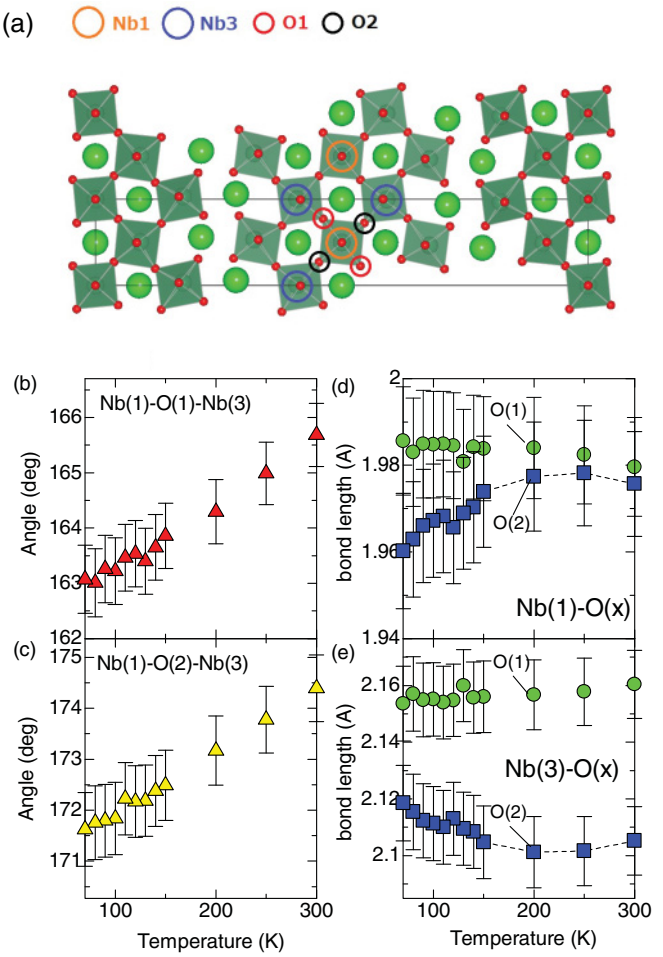

FIG. 6. (Color online) (a) Projection along the a axis of $SrNbO_{3.43}$. Temperature dependences of bond lengths of (a) Nb(1)-O(x) ($x = 1,2$) and (b) Nb(3)-O(x) ($x = 1,2$) and bond angles of (c) Nb(1)-O(1)-Nb(3) and (d) Nb(1)-O(2)-Nb(3).

referring to Fig. 6(a). At 300 K, the Nb(1)-O(1) bond length is equal to the Nb(1)-O(2) bond length, which shows that $Nb(1)O_6$ is a perfect octahedron. On the other hand, the Nb(1)-O(1) bond length is significantly larger than the Nb(1)-O(2) bond length at 80 K, reflecting a distortion of the $Nb(1)O_6$ octahedron [see Fig. 6(a)]. Correspondingly, the difference between the Nb(3)-O(1) and the Nb(3)-O(2) bond lengths becomes smaller with decreasing temperature, which shows that the $Nb(3)O_6$ octahedron starts to release its distortion with decreasing temperature [see Fig. 6(a)]. As described above, the distortion-released $Nb(3)O_6$ octahedron may contribute to the transport better than the distorted ones, which will realize rather isotropic conduction in the ab plane. In fact, the anisotropy in resistivity in the ab plane seems to decrease with decreasing temperature as shown in Fig. 3(a). Thus, it seems that electric transport is affected by transforming NbO_6 octahedra to be stable in higher dimensional transport. In other words, dimensional crossover might occur below 150 K. Such dimensional crossover is universally observed in Q1D materials, where the interchain hopping energy is finite. Finite interchain hopping will induce warping of the Fermi surface and effect 2D or 3D behavior below $t_\perp$ ($t_\perp$: interchain hopping energy).[29,34] Naive thinking suggests that the higher dimensionality will induce a metallic state rather than an insulating state.

Finally, we would like to emphasize the unique transport properties in $SrNbO_{3.43}$; a high anisotropy in the thermopower appears at T^*, which is related to the dimensional crossover from a higher dimensional to a Q1D electronic structure associated with the shapes of $Nb(1)O_6$ and $Nb(3)O_6$ octahedra. Though Q1D material generally shows a high anisotropy in thermopower, there is no example that exhibits both the low thermopower that is typical for a conventional metal and the high thermopower typical for a semiconductor except for $SrNbO_{3.43}$, as far as we know. Thanks to the enhanced thermopower along the b axis, the ZT along the b axis is the largest of the ZTs along all the crystallographic axes. These results show that the Q1D electronic structure enhances the thermopower even in a bulk crystal.

IV. CONCLUSION

We have systematically investigated the transport properties of a $SrNbO_{3.43}$ single crystal along all crystallographic axes. The resistivity, thermopower, and thermal conductivity were found to be highly anisotropic, which reflects Q1D electronic

and crystal structures. In particular, the thermopower along the b axis is -170 μV/K, which is 1 order of magnitude higher than the -15 and -25 μV/K along both the a and the c axes. A high anisotropy in the thermopower appears at T^*, which is related to the dimensional crossover from a higher dimensional to a Q1D electronic structure associated with the shapes of $Nb(1)O_6$ and $Nb(3)O_6$ octahedra.

ACKNOWLEDGMENTS

We appreciate the technical support of Y. Nakahara and S. Vasala. This study has been approved by the Photon Factory Program Advisory Committee (Proposal No. 2009S2-008). This work was partially supported by the Strategic Japan–Finland Cooperative Program on "Functional Materials," JST, Japan.

*kobayashi.wataru.gf@u.tsukuba.ac.jp

[1] L. D. Hicks and M. S. Dresselhaus, Phys. Rev. B **47**, 16631 (1993).

[2] M. S. Dresselhaus, G. Chen, M. Y. Tang, R. G. Yang, H. Lee, D. Z. Wang, Z. F. Ren, J.-P. Fleurial, and P. Gogna, Adv. Mater. **19**, 1043 (2007).

[3] R. Venkatasubramanian, E. Siivola, T. Colpitts, and B. O'Quinn, Nature **413**, 597 (2001).

[4] A. I. Hachbaum, R. Chen, R. D. Delgado, W. Liang, E. C. Garnett, M. Najarian, A. Majumdar, and P. Yang, Nature **451**, 163 (2008).

[5] A. I. Boukai, Y. Bunimovich, J. Tahir-Kheli, J.-K. Yu, W. A. Goddard III, and J. R. Heath, Nature **451**, 168 (2008).

[6] H. Ohta, S. Kim, Y. Mune, T. Mizoguchi, K. Nomura, S. Ohta, T. Nomura, Y. Nakanishi, Y. Ikuhara, M. Hirano, H. Hosono, and K. Koumoto, Nature Mater. **6**, 129 (2007).

[7] I. Terasaki, Y. Sasago, and K. Uchinokura, Phys. Rev. B **56**, R12685 (1997).

[8] K. Fujita, T. Mochida, and K. Nakamura, Jpn. J. Appl. Phys. **40**, 4644 (2001).

[9] R. Funahashi, I. Matsubara, H. Ikuta, T. Takeuchi, U. Mizutani, and S. Sodeoka, Jpn. J. Appl. Phys. **39**, L1127 (2000).

[10] D. J. Singh, Phys. Rev. B **61**, 13397 (2000).

[11] K. Kuroki and R. Arita, J. Phys. Soc. Jpn. **76**, 083707 (2007).

[12] W. Koshibae, K. Tsutsui, and S. Maekawa, Phys. Rev. B **62**, 6869 (2000).

[13] M. Mikami, R. Funahashi, M. Yoshimura, Y. Mori, and T. Sasaki, J. Appl. Phys. **94**, 6579 (2003).

[14] A. Maignan, S. Hébert, C. Martin, and D. Flahaut, Mater. Sci. Eng. **104**, 121 (2003).

[15] K. Iwasaki, T. Yamamoto, H. Yamane, T. Takeda, S. Arai, H. Miyazaki, K. Tatsumi, M. Yoshino, T. Ito, Y. Arita, S. Muto, T. Nagasaki, and T. Matsui, J. Appl. Phys. **106**, 034905 (2009).

[16] W. Kobayashi, S. Hébert, O. Pérez, D. Pelloquin, and A. Maignan, Phys. Rev. B **79**, 085207 (2009).

[17] W. Kobayashi, Phys. Rev. B **79**, 155116 (2009).

[18] A. Pautrat and W. Kobayashi, Phys. Rev. B **82**, 115113 (2010).

[19] C. A. Kuntscher, S. Schuppler, P. Haas, B. Gorshunov, M. Dressel, M. Grioni, F. Lichtenberg, A. Hernberger, F. Mayr, and J. Mannhart, Phys. Rev. Lett. **89**, 236403 (2002).

[20] S. C. Abrahams, H. W. Schmalle, T. Williams, A. Reller, F. Lichtenberg, D. Widmer, J. G. Bednorz, R. Spreiter, Ch. Bosshard, and P. Günter, Acta Crystallogr. Sec. B **54**, 399 (1998).

[21] A. Sakai, T. Kanno, K. Takahashi, Y. Yamada, and H. Adachi, J. Appl. Phys. **108**, 103706 (2010).

[22] F. Lichtenberg, A. Herrnberger, K. Wiedenmann, and J. Mannhart, Prog. Solid State Chem. **29**, 1 (2001).

[23] A. de Campos, M. S. da Luz, C. A. M. dos Santos, A. T. Rice, A. M. Deml, B. D. White, J. J. Neumeier, and J. L. Cohn, Phys. Rev. B **82**, 125117 (2010).

[24] F. Lichtenberg, T. Williams, A. Reller, D. Widmer, and J. G. Bednorz, Z. Phys. B **84**, 369 (1991).

[25] K. Mortensen, Solid State Commun. **44**, 643 (1982).

[26] L. Chaput, G. Hug, P. Pécheur, and H. Scherrer, Phys. Rev. B **71**, 121104 (2005).

[27] J. M. Ziman, *Principles of the Theory of Solids*, 2nd ed. (Cambridge University Press, Cambridge, 1979).

[28] S. Okada, I. Terasaki, H. Ooyama, and M. Matoba, J. Appl. Phys. **95**, 6816 (2004).

[29] I. Terasaki, N. Seiji, S. Adachi, and H. Yamauchi, Phys. Rev. B **54**, 11993 (1996).

[30] B. Yang, W. L. Liu, J. L. Liu, K. L. Wang, and G. Chen, Appl. Phys. Lett. **81**, 3588 (2002).

[31] A. Smontara, I. Tkalčec, A. Bilušić, M. Budimir, and H. Berger, Physica B **316-317**, 279 (2002).

[32] H. Winter, S. Schuppler, and C. A. Kuntscher, J. Phys. Condens. Matter **12**, 1735 (2000).

[33] C. A. Kuntscher, S. Gerhold, N. Nücker, T. R. Cummins, D.-H. Lu, S. Schuppler, C. S. Gopinath, F. Lichtenberg, J. Mannhart, and K.-P. Bohnen, Phys. Rev. B **61**, 1876 (2000).

[34] T. Giamarchi, Chem. Rev. **104**, 5037 (2004).